Anal. Chem. **2007,** *79,* 3575−3580

Modification of Trapping Potential by Inverted Sidekick Electrode Voltage during Detection To Extend Time-Domain Signal Duration for Significantly Enhanced Fourier Transform Ion Cyclotron Resonance Mass Resolution

Sunghwan Kim, Myoung Choul Choi, Seungyoung Kim, Manhoi Hur, Hyun Sik Kim,* and Jong Shin Yoo*

Korea Basic Science Institute, 113 Gwahangno, Yusung-Gu, Daejeon 305-333, Republic of Korea

Greg T. Blakney, Christopher L. Hendrickson, and Alan G. Marshall

Ion Cyclotron Resonance Program, National High Magnetic Field Laboratory, Florida State University, 1800 East Paul Dirac Drive,Tallahassee, Florida 32310-4005

Applying an inverted voltage to the "sidekick" electrodes during ion cyclotron resonance detection improves both Fourier transform ion cyclotron resonance (FT-ICR) mass spectral signal-to-noise ratio (at fixed resolving power) and resolving power (at fixed signal-to-noise ratio). The time-domain signal duration increases by up to a factor of 2. The method has been applied to 7-T FT-ICR MS of electrosprayed positive ions from substance P and human growth hormone protein (~22 000 Da, $m/\Delta m_{50\%}$ 200 000), without the need for pulsed cooling gas inside the ICR trap. The modification can be easily adapted to any FT-ICR instrument equipped with sidekick electrodes. The present effects are shown to be comparable to electron field modification by injection of an electron beam during ICR detection, reported by Kaiser and Bruce (Kaiser, N. K.; Bruce, J. E. ***Anal. Chem.*** **2005, 77, 5973−5981.). Although the exact mechanism is not fully understood, computer simulations show that a flattening of the radial potential gradient along the magnetic field direction in the ICR trap may contribute to the effects. This study not only provides a way to enhance the quality of FT-ICR mass spectra but also offers insight into understanding of ion motions inside an ICR ion trap.**

Since its inception,[2] Fourier transform ion cyclotron resonance mass spectrometry (FT-ICR MS) has become the ultimate standard for high-resolution broadband mass analysis.[3] Resolving power of 3 300 000 for a ~1-kDa peptide has been reported with this technique.[4] The high-resolution capability of FT-ICR MS has had high impact on protein and natural organic mixture analysis.[5−11]

Resolving power in FT-ICR MS is limited by the duration of the time-domain ICR signal.[3] Therefore, there have been several approaches to improve trap design[12−18] and to better understand ion motion.[19,20] Ideally, a Penning trap[21] confines and stores ions by combination of a spatially uniform static magnetic field and a three-dimensional axial quadrupolar electrostatic field. The quadrupolar field ensures that the ion cyclotron frequency is independent of ion location in the trap. Ions in such a trap exhibit three periodic motions (cyclotron rotation, magnetron rotation, and axial "trapping" oscillation).[22] Ion stability derives from these motions. Cyclotron rotation results from the Lorentz force on an ion of mass, m, and charge, q, moving in a static magnetic field,

* Corresponding authors. E-mail: jongshin@kbsi.re.kr. fticr@kbsi.re.kr.

(1) Kaiser, N. K.; Bruce, J. E. *Anal. Chem.* **2005**, *77*, 5973−5981.
(2) Comisarow, M. B.; Marshall, A. G. *Chem. Phys. Lett.* **1974**, *25*, 282−283.
(3) Marshall, A. G.; Hendrickson, C. L.; Jackson, G. S. *Mass Spectrom. Rev.* **1998**, *17*, 1−35.
(4) He, F.; Hendrickson, C. L.; Marshall, A. G. *Anal. Chem.* **2001**, *73*, 647−650.
(5) Zhang, L. K.; Rempel, D.; Pramanik, B. N.; Gross, M. L. *Mass Spectrom. Rev.* **2005**, *24*, 286−309.
(6) Kelleher, N. L. *Anal. Chem.* **2004**, *76*, 196A-203A.
(7) He, F.; Emmett, M. R.; Hakansson, K.; Hendrickson, C. L.; Marshall, A. G. *J. Proteome Res.* **2004**, *3*, 61−67.
(8) McLafferty, F. W. *Int. J. Mass Spectrom.* **2001**, *212*, 81−87.
(9) Masselon, C.; Anderson, G. A.; Harkewicz, R.; Bruce, J. E.; Pasa-Tolic, L.; Smith, R. D. *Anal. Chem.* **2000**, *72*, 1918−1924.
(10) Hughey, C. A.; Rodgers, R. P.; Marshall, A. G. *Anal. Chem.* **2002**, *74*, 4145−4149.
(11) Kim, S.; Kramer, R. W.; Hatcher, P. G. *Anal. Chem.* **2003**, *75*, 5336−5344.
(12) Vandyck, R. S.; Wineland, D. J.; Ekstrom, P. A.; Dehmelt, H. G. *Appl. Phys. Lett.* **1976**, *28*, 446−448.
(13) Gabrielse, G. *Phys. Rev. A* **1983**, *27*, 2277−2290.
(14) Gabrielse, G.; Mackintosh, F. C. *Int. J. Mass Spectrom. Ion Processes* **1984**, *57*, 1−17.
(15) Naito, Y.; Fujiwara, M.; Inoue, M. *Int. J. Mass Spectrom. Ion Processes* **1992**, *120*, 179−192.
(16) Vartanian, V. H.; Hadjarab, F.; Laude, D. A. *Int. J. Mass Spectrom.* **1995**, *151*, 175−187.
(17) Gooden, J. K.; Rempel, D. L.; Gross, M. L. *J. Am. Soc. Mass Spectrom.* **2004**, *15*, 1109−1115.
(18) Guan, S. H.; Marshall, A. G. *Int. J. Mass Spectrom. Ion Processes* **1995**, *146*, 261−296.
(19) Chen, R.; Guan, S.; Marshall, A. G. *J. Chem. Phys.* **1994**, *100*, 2258−2266.
(20) Guan, S.; Xiang, X.; Marshall, A. G. *Int. J. Mass Spectrom. Ion Processes* **1993**, *124*, 53−67.
(21) Penning, F. M. *Physica* **1936**, *3*, 873.
(22) Brown, L. S.; Gabrielse, G. *Rev. Mod. Phys.* **1986**, *58*, 233−311.

10.1021/ac062016z CCC: $37.00
Published on Web 04/20/2007

B_0, and prevents ions from escaping in directions perpendicular to B_0. In the absence of an electric field the ion cyclotron angular frequency, ω_c, is given by

$$\omega_c = qB_0/m \quad \text{(“unperturbed” cyclotron frequency, SI units)} \quad (1)$$

The quadrupolar trapping potential has three effects. First, it introduces a sinusoidal “trapping” axial oscillation along B_0, at frequency, ω_z, thereby preventing ions from escaping along the (axial) B_0 direction. Second, the cyclotron frequency is shifted (downward) from ω_c to ω_+. Finally, there is a new “magnetron” rotation perpendicular to B, at frequency, ω_-.[22]

$$\omega_z = \sqrt{\frac{2\,qV_{trap}\alpha}{ma^2}} \quad \text{(“trapping” oscillation frequency, in SI units)} \quad (2)$$

$$\omega_+ = \frac{\omega_c}{2} + \sqrt{\left(\frac{\omega_c}{2}\right)^2 - \left(\frac{\omega_z}{2}\right)^2} \quad \text{(“reduced” cyclotron frequency)} \quad (3)$$

$$\omega_- = \frac{\omega_c}{2} - \sqrt{\left(\frac{\omega_c}{2}\right)^2 - \left(\frac{\omega_z}{2}\right)^2} \quad \text{(“magnetron” frequency)} \quad (4)$$

in which a is a characteristic measure of the trap length and α depends on the trap geometry.[3] Magnetron motion results from the radial electric field generated by the electrostatic trapping potential.

In a typical closed cylindrical ICR cell, the radial electric field is directed outward toward the excitation and detection electrodes. The resulting outward radial force destabilizes ions, because the ion magnetron radius increases as ions lose energy by ion−neutral or ion−ion collisions, ultimately leading to radial ejection and limiting the length of time that ions can be held in the trap.

It is important to note that eqs 2−4 are derived only for a perfectly quadrupolar electrostatic trapping potential. That assumption is valid only near the center of a trap and in the absence of other ions. Under those conditions, the three “natural” ion motions are virtually independent[23] and ions can be confined for a long period of time without significant loss (the record is 10 months for a single electron in a Penning trap.[24]) However, collisions with neutrals,[25] deviation from quadrupole electrostatic trapping potential due to truncated or otherwise imperfect trapping electrodes, or Coulombic charge interactions[26] can destabilize ions radially and result in damping of the time-domain ICR signal. Mathematically, higher order terms must be added to the quadrupolar electrostatic potential. Under either of the described conditions, the three ion motions are no longer independent.

Here, we demonstrate experimentally that a simple modification of the trapping potential can significantly improve mass resolving power in FT-ICR MS. The modification is achieved simply by applying a negative voltage to the “sidekick” electrode after ion excitation in detection of positive ions. We offer qualitative discussion, supported by computer simulation, to account for the improvement and to relate it to similar recent resolution enhancement based on introduction of an axial electron beam during ICR signal detection.[1]

EXPERIMENTAL METHODS

Agilent tuning mix, substance P purchased from Sigma Aldrich, and human growth hormone (LG Life Science) served as standard samples. Samples were electrosprayed by direct injection at 1−10 μM in 50:50 v/v water/methanol solution with 0.5−1% formic acid at a flow rate of ~300 nL/min through a homemade 50-μm-i.d. fused-silica needle spray tip at ground, with negative voltage (−1.5 to 2.5 kV) on the front electrode of the glass capillary. Ion desolvation was aided by heated gas flow.

A Bruker Daltonics APEX-Q70 system controlled by a Predator data station[27] was used to generate FT-ICR mass spectra. The Predator data acquisition system includes 17 channels of analog voltage (±10 V, 16 16-bit voltages, and 1 12-bit voltage), 18 TTL triggers, and a 6-channel high-power dc voltage amplifier (±200 V). Connection of the Predator to the APEX-Q70 instrument is described elsewhere.[28] With that data station, all functions of the commercial instrument can be controlled. In addition, the data station is flexible so that most of the FT-ICR MS experimental parameters may be adjusted for each experimental event sequence. The APEX-Q70 (7 T) system is equipped with an Infinity cell.[29] The Infinity cell is composed of two trap plates (front and back traps), sidekick electrodes (refer to Figure 1), and excitation and detection plates (see Figure 1). The arrows indicating “ion motion” are presented here to give an idea of the direction of trapping motion only. Lengths of the arrows do not represent actual amplitude of the motion. The experimental event sequence is illustrated in Figure 2. Briefly, ions are accumulated in a hexapole collision cell for 0.1−1 s according to analyte concentration. Ions are transported to the ICR trap during a transfer period of 1.6−2.0 ms and captured in the ICR trap by lowering the front (entrance) end cap voltage and raising the back end cap voltage.

In conventional (normal) operation, the sidekick electrodes are held at the same voltage as the end cap electrodes during ion detection. Shortly (2.0 ms) after ions enter the ICR trap, the front end cap voltage is raised to 4 V to hold ions in the ICR cell. Ions were excited to 30−50% of the cell diameter by broadband frequency-sweep (chirp) dipolar excitation (25−539 kHz at a sweep rate of 100−250 Hz/μs). Direct mode image current detection was performed to yield time-domain data. Time-domain data sets (512k−8M data points) were coadded to enhance signal-to-noise ratio (10−20 acquisitions) and then Hanning apodized, followed by one zero-fill before fast Fourier transformation and magnitude calculation.

(23) Horvath, G. Z. K.; Hernandez-Pozos, J. L.; Dholakia, K.; Rink, J.; Segal, D. M.; Thompson, R. C. *Phys. Rev. A* **1998**, *57*, 1944−1956.
(24) Gabrielse, G.; Dehmelt, H.; Kells, W. *Phys. Rev. Lett.* **1985**, *54*, 537−539.
(25) Guan, S. H.; Li, G. Z.; Marshall, A. G. *Int. J. Mass Spectrom.* **1997**, *167*, 185−193.
(26) Mitchell, D. W.; Smith, R. D. *Phys. Rev. E* **1995**, *52*, 4366−4386.
(27) Blakney, G. T.; Lam, T. T.; Hendrickson, C. L.; Marshall, A. G. Proc. 52th Am. Soc. Mass Spectrom. Conf. Mass Spectrom. Allied Top., American Society for Mass Spectrometry, Nashville, TN, 2004.
(28) Kim, S. Y.; Yoo, J. S.; Blakney, G. T.; Hendrickson, C. L.; Marshall, A. G.; Kim, H. S. Proc. 53rd Am. Soc. Mass Spectrom. Conf. Mass Spectrom. Allied Top. American Society for Mass Spectrometry, San Antonio, TX, June 6, 2005; 2005; TP 219.
(29) Caravatti, P.; Allemann, M. *Org. Mass Spectrom* **1991**, *26*, 514−518.

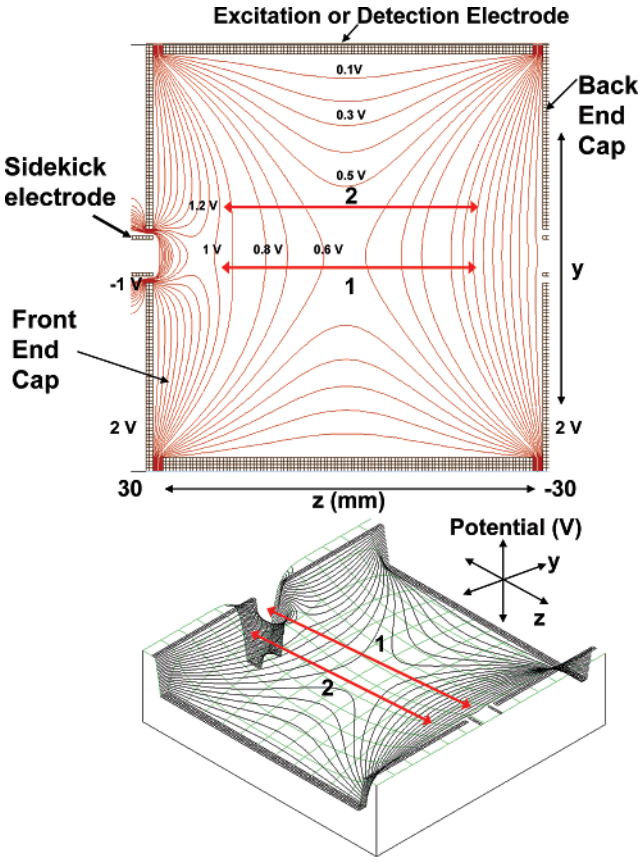

Figure 1. Simulated dc potential in the *yz* plane of an ICR cell. Top: two-dimensional isopotential contours. Bottom: three-dimensional display showing isopotential lines. End cap potentials are 2 V, and the sidekick electrode is at −1 V. The magnetic field is along the *z*-axis. The negative sidekick electrode creates a trough along the cell *z*-axis. Although ions moving along line 1 will be ejected axially; ions excited to 33% of the cell radius (line 2) oscillate between the end caps and remain trapped.

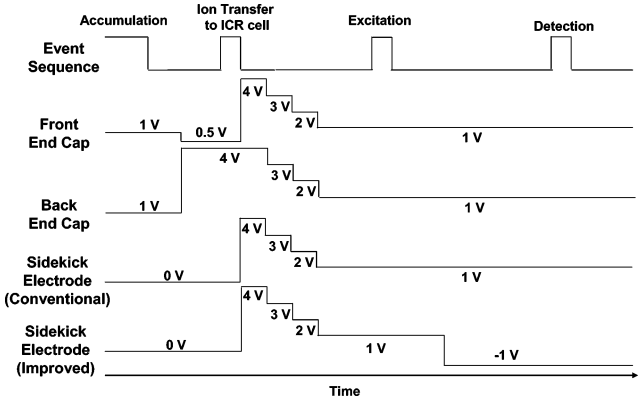

Figure 2. Experimental event sequence (top, not to scale) and voltages for front and back end cap electrodes and sidekick electrode.

Computer simulations were performed with SIMION 3D version 7 running on a 3.1-GHz Pentium 4 PC with 2-GB RAM. A model cell for simulation had 60-mm length and an inner diameter of 60 mm. The model was defined by small grid size (0.5 mm/gu) and then refined down to a convergence level of 10^{-5}. So-called electron-promoted ion coherence[1] was achieved by passing through the ICR cell an axial electron beam generated by a hollow cathode emitter[30] during ICR detection. A bias voltage was used

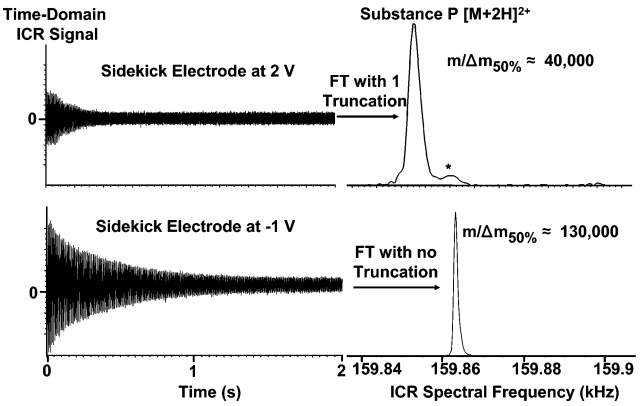

Figure 3. Time-domain (left) and frequency-domain (right) ICR signals, for electrosprayed substance P, detected with end cap electrodes at 2 V and sidekick voltage at 2 (top) or −1 V (bottom) during detection. Note that mass resolving power ($m/\Delta m_{50\%}$) and frequency resolving power ($\omega/\Delta\omega_{50\%}$) in FT-ICR MS are identical.[3]

to regulate electron flow through the ICR cell. The voltage was normally set at 1 V and switched to −0.5 to −1.3 V to generate the axial electron beam. The current-controlled cathode was operated at 1.9 mA.

RESULTS AND DISCUSSION

Positive versus Negative Sidekick Electrode Voltage during ICR Detection. Sidekick electrodes improve ion trapping efficiency by deflecting ions away from the central axis, so that incident ions cannot pass back through the front end cap aperture after reflection from the back end cap electrode. However, the deflected ions can acquire a significant magnetron radius, adversely affecting on-axis IRMPD analysis.[31] We therefore typically employ gated trapping, whereby the sidekick electrodes are held at the same voltage as the front trapping electrode (Figure 2, "conventional" mode).

However, we found that the time-domain ICR signal duration could be significantly extended by switching the sidekick electrode potential to a negative voltage (for positive ions) after excitation (Figure 2, "improved" mode). Time-domain ICR signals obtained with positive and negative sidekick voltage (during detection) are displayed in Figure 3. All other experimental conditions were identical. The detected image current scale is the same in both plots. For sidekick voltage (during detection) equal to the end cap voltage, the time-domain ICR signal is relatively low in amplitude and lasted only for a couple hundred milliseconds (Figure 3, upper left). However, lowering the sidekick voltage to −1 V during detection increased both the amplitude and duration (more than 2 s) of the time-domain ICR signal (Figure 3, lower left). Both time-domain signals were Hanning apodized, zero-filled, and Fourier transformed. To display a similar signal-to-noise ratio, the time-domain signal obtained with 2-V sidekick voltage (during detection) was truncated by half before Fourier transformation. Mass spectral resolving power, $m/\Delta m_{50\%}$ (in which $\Delta m_{50\%}$ is the peak full width at half-maximum peak height) improved more than 3-fold (from 40 000 to 130 000). Application of a negative voltage

(30) Tsybin, Y. O.; Witt, M.; Baykut, G.; Kjeldsen, F.; Hakansson, P. *Rapid Commun. Mass Spectrom.* **2003**, *17*, 1759−1768.
(31) Hofstadler, S. A.; Sannes-Lowery, K. A.; Griffey, R. H. *Rapid Commun. Mass Spectrom.* **2001**, *15*, 945−951.

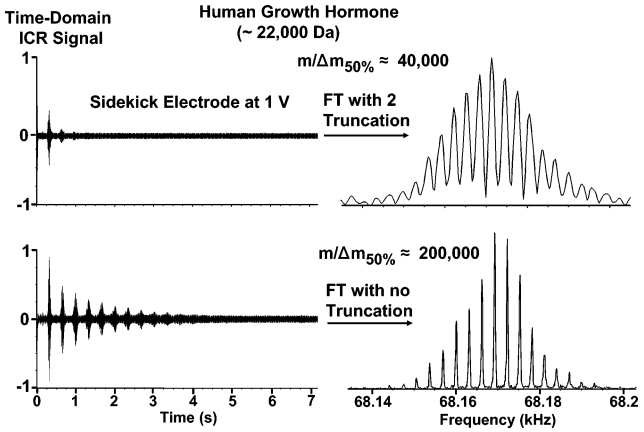

Figure 4. Time-domain (left, same vertical scale in both plots) and frequency-domain (right) ICR signals, for electrosprayed positive ions of human growth hormone protein (monoisotopic neutral mass 22 115.072 Da), detected with end cap electrodes at 1 V and sidekick voltage (during detection) at 1 (top) or −1 V (bottom) during detection.

(up to −2 V, not shown) did not reduce ion trapping efficiency. It could be because the ions are at a radius at which the sidekick voltage (during detection) has minimal impact on axial potential. The time-domain signal initial amplitudes are significantly different for the two data sets shown in Figure 3, even though experimental conditions other than the sidekick voltage during detection were the same. Thus, the difference in signal amplitude must be due to additional postexcitation ion loss at 2 V sidekick voltage.

Figure 4 shows that the salutary effects of the negative sidekick voltage (during detection) also extend to the analysis of human growth hormone protein (monoisotopic neutral mass, 22 115.072 Da) with increased time-domain signal duration (from 1.5 to 7 s) and correspondingly 5-fold improvement in resolving power when same signal-to-noise ratio of FT-ICR signal was maintained.

Effect of ICR Trap Axial Position. The two top panels in Figure 5 show the improvement in time-domain ICR signal duration (for substance P) due to changing only the sign of the sidekick potential (from +1 V to −1 V). However, because the negative voltage is applied to only one end of the ICR trap, the center of trapping oscillation will be shifted axially toward the front end cap electrode by a few millimeters, and thus away from the central magnetic field. We therefore displaced the ICR trap by ~3 mm to shift the center of the trapping oscillation back to the magnetic field center. The resulting time-domain ICR signals for +1 and −1 V sidekick electrode voltage (Figure 5, bottom panels) showed essentially the same trend of improvement as those in Figure 5, top panels. Thus, the axial asymmetry in trapping potential introduced by negative sidekick electrode voltage does not appear to impact the data.

Effect of Negative Sidekick Voltage during Excitation/Detection versus Detection Only. It is intuitively reasonable to expect that ion trapping efficiency could be negatively affected by distortion of the trapping field by application of a negative sidekick electrode voltage. Figure 6 shows that application of a negative sidekick electrode voltage during excitation as well as detection reduces FT-ICR mass spectral signal-to-noise ratio by more than half compared to the signal acquired for negative sidekick voltage applied only during detection. The reason is presumably that the distortion in trapping potential is greatest

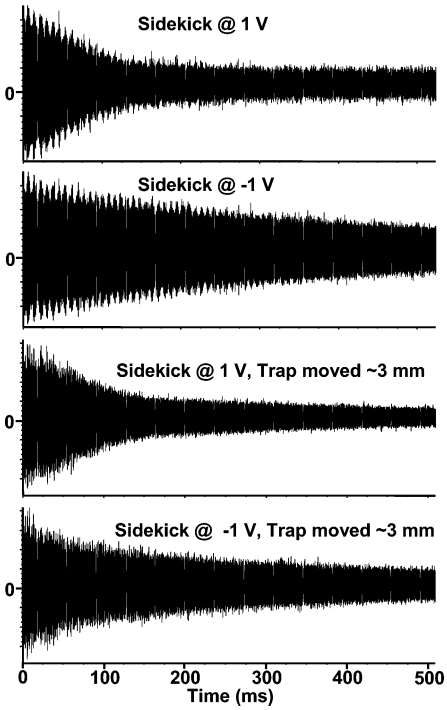

Figure 5. Effect of sidekick voltage (during detection) and cell position on the ICR signal from substance P. End cap voltage is 1 V in each case.

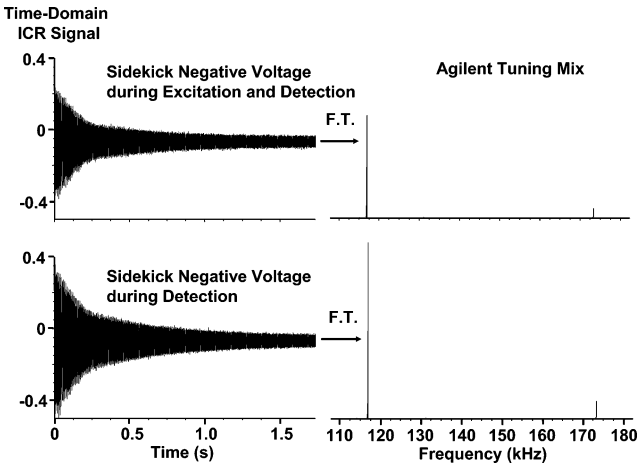

Figure 6. Effect of negative sidekick voltage applied during both excitation and detection (top) or just during detection (bottom), for electrosprayed (positive ions) Agilent tuning mix.

near the trap axis and thus affects ions more during excitation (during which ions are initially close to that axis) than detection (during which ions have expanded ICR orbital radius and are thus farther from the axis).

Simulated Trapping Potential in the Presence and Absence of Sidekick Electrode Voltage. Figure 1 shows the electrostatic isopotential contours (Simion version 7.0) inside an ICR trap configured with sidekick electrodes. Imposition of a negative sidekick voltage (during detection) forms an axial potential valley. Positive ions initially on-axis will be axially ejected at the front end cap electrode (path 1 in Figure 1). However, the trap potential at 33% of the trap radius (e.g., after ion excitation) is only slightly distorted by negative sidekick potential, so that ions oscillate between the front and back end cap electrodes (path 2 in Figure 1). Figure 1 thus explains why a negative sidekick

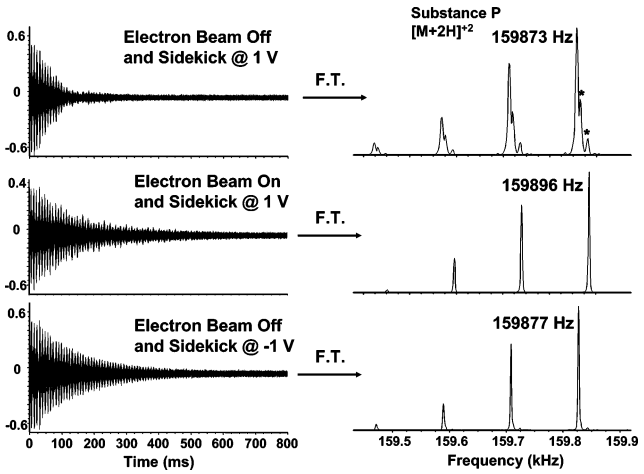

Figure 7. Effects of electron beam and negative sidekick voltage (during detection) on time-domain (left) and frequency-domain (right) ICR signals for electrosprayed substance P. '*' denotes sidebands.

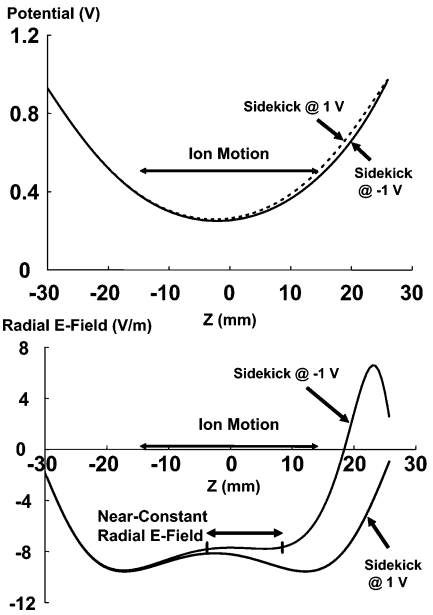

Figure 8. Simulated potential (top) and radial electric field (bottom) at 33% of the trap radius) in an ICR trap with sidekick voltage (during detection) at 1 or −1 V. The end cap potentials are 1 V.

potential affects ions during excitation (initially small ICR radius) but not during detection (large ICR radius).

Effect of an Axial Electron Beam during ICR Detection. Kaiser and Bruce recently reported that the introduction of an on-axis electron beam during ICR detection can significantly increase the time-domain ICR signal duration (and thus enhance FT-ICR MS resolving power).[1] We have repeated their experiment to compare its effect to that of applying a negative sidekick electrode voltage during detection. Figure 7 shows FT-ICR mass spectra of substance P under three conditions: sidekick voltage (during detection) set at the same voltage (+1 V) as the front end cap electrode and dispenser cathode bias voltage set so that no electrons enter the cell (Figure 7, top); sidekick electrode voltage at +1 V, with electrons injected throughout the ion detection period (Figure 7 middle); and sidekick electrode voltage at −1 V, with no injected electrons (Figure 7, bottom). Clearly, either the electron beam or the negative sidekick electrode voltage results in increased time-domain ICR signal duration and corresponding enhancement in FT-ICR MS signal-to-noise ratio and resolving power. The ICR frequencies also increased in both cases, due to decrease in the magnitude of the electrostatic trapping potential (see eqs 2 and 3). Reduced trapping frequency term in eq 2 will contribute to increased observed frequency (ω_+).

Elimination of Sideband Signals. Another benefit from either electron beam or negative sidekick electrode voltage is the decrease or disappearance of sidebands (asterisks in Figure 3 and Figure 7, top) in FT-ICR mass spectra. The frequency differences between sidebands and the main peak are less than 15 Hz and agree well with the magnetron frequency calculated from eq 4.

SIMION Simulations of Electrostatic Potential. The electrostatic potential and radial electric field at a typical postexcitation ion cyclotron radius (33% of the trap radius, path 2 in Figure 1) as a function of axial position, z, are shown in Figure 8. The "ion motion" arrows in Figure 8 indicate the direction (but not amplitude) of axial oscillation. Applying a negative voltage to the sidekick electrodes changes the electrostatic potential only slightly (by up to 6%—see Figure 8, top) due to the radial distance from the sidekick electrode and its smaller physical diameter (6 mm) compared to that of the front end cap (60 mm).

The change in radial potential gradient due to +1 or −1 V sidekick voltage (during detection) is more significant (Figure 8, bottom). In a perfectly quadrupolar electrostatic trapping potential, the radial electric field increases linearly with increasing r but is independent of z. In the actual trap of Figure 1, application of +1 V to the sidekick electrodes generates a double-well radial electric field as a function of z, whereas application of −1 V to the sidekick electrodes raises the bottom of one of those wells by ~25%, so that the radial electric field becomes essentially independent of z near the trap midplane (−3 mm < z < 10 mm) and at 33% of the trap radius (Figure 8, bottom). In that respect, the negative sidekick electrode voltage is similar to a screened trap[32] or a trap with interlacing "comb" wires as rf end cap electrodes,[33] both of which effectively produce near-zero (and thus constant) radial electric field as a function of z.

In other words, ions subjected to negative sidekick electrode voltage encounter an electrostatic trapping potential that closely approximates quadrupolar, at 33% of cell radius and near the trap midplane (−3 mm < z < 10 mm). In summary, applying a negative voltage to the sidekick electrodes offers yet another approach to tailoring the electrostatic trap potential for enhanced signal-to-noise ratio or mass resolving power.[12−15,17,25,34]

Finally, it should be noted that negative sidekick voltage (during detection) did not always increase signal duration in our experiments. If ions were excited to ~15% of the trap radius, the time-domain signal lasted longest if the sidekick voltage (during detection) was held at the same voltage as the end cap electrodes. Negative sidekick electrode voltage during detection improved the FT-ICR mass spectral signal-to-noise ratio only if ions were excited to a radius larger than 15% of the trap radius (we typically excite to 33% of the trap radius). Moreover, negative sidekick

(32) Wang, M.; Marshall, A. G. *Anal. Chem.* **1989**, *61*, 1288−1293.
(33) Franzen, J.; Nikolaev, E. Bruker Daltonik GmbH, Application Note 11/197129, 2006.
(34) Vartanian, V. H.; Laude, D. A. *Int. J. Mass Spectrom.* **1998**, *178*, 173−186.

electrode voltage (during detection) offered only marginal extension of the time-domain signal for a mixture of ions with many different m/z exits (e.g., petroleum). This effect cannot be explained by single-ion behavior and is likely due to increased ion−ion interactions with increased number of trapped ions. Further understanding will likely require large-scale numerical simulation of ion cloud behavior in the trap.[35]

CONCLUSION

We have shown that applying a negative voltage to the sidekick electrodes during ICR detection can significantly improve FT-ICR mass spectral signal-to-noise ratio, mass resolving power, or both. The effects of the present modification are similar to those resulting from injection of an electron beam during ICR detection, reported by Kaiser and Bruce.[1] Advantages of the present method are (a) optimization is easier because the electrostatic potential can be more finely controlled and (b) there is no heating and increase in pressure in the ion trap due to the proximity of the dispenser cathode electron emitter.

(35) Nikolaev, E. N. 17th Int. Mass Spectrom. Conf., Prague, Czech Republic, 27 Aug−1 Sep 2006; p 285.

In the current configuration of the ICR trap, modification can be done at only one end of the trap. It is reasonable to expect that symmetric trap potential modification on both ends of the trap could be even more beneficial. Moreover, similar trap potential modification could be applied to other ICR ion trap geometries.

ACKNOWLEDGMENT

We thank John P. Quinn for help in interfacing the Predator data station to the Bruker FT-ICR mass spectrometer. We also thank Dr. Jung-Keun Suh and Young-Lan Jung for providing protein standard samples. This work was supported by KBSI JUMP project "Development of an FT-ICR instrument", the NSF National High Field FT-ICR Facility (DMR-00-84173), Florida State University, and the National High Magnetic Field Laboratory in Tallahassee, FL.

Received for review October 27, 2006. Accepted March 9, 2007.

AC062016Z